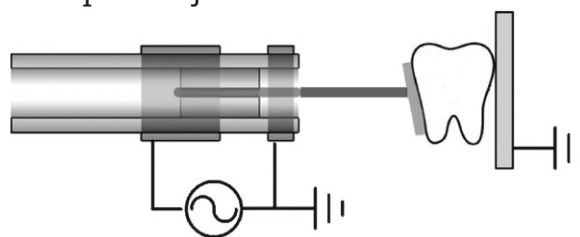


# Atmospheric Pressure Plasma Jet Composed of Three Electrodes: Application to Tooth Bleaching

Hyun Woo Lee, Seoul Hee Nam, Abdel-Aleam H. Mohamed,  
Gyoo Cheon Kim,\* Jae Koo Lee

Three-electrode plasma jet system consisting of a perforated dielectric tube with two outer and one floating inner electrodes was developed and employed for tooth bleaching. Lowered gas breakdown voltage and increased discharge current were achieved by using the floating inner electrode. Optical emission spectra analysis showed that the rotational temperature of the second positive nitrogen bands was  $\approx 290$  K and vibrational temperature was  $\approx 2500$  K, which means this plasma is in highly non-equilibrium state and nonthermal. The presence of excited He,  $N_2$ ,  $N_2^+$  and O in the plasma plume was revealed. The plasma jet was used in combination with hydrogen peroxide ( $H_2O_2$ ) to remove stains from extracted teeth stained by either coffee or red wine. Combining the plasma jet and  $H_2O_2$  improved the bleaching efficacy by a factor of 3.1 (coffee) and 3.7 (red wine) compared with using  $H_2O_2$  alone.



## Introduction

Non-equilibrium atmospheric pressure plasmas have potential for biomedical applications because they are nonthermal and nontoxic, and because they have the

potential to be realized in hand-held devices.<sup>[1–3]</sup> Non-equilibrium atmospheric pressure plasmas have been used for biomedical applications, such as sterilization,<sup>[4]</sup> blood coagulation,<sup>[5]</sup> wound healing<sup>[6]</sup> and even cancer treatment.<sup>[7]</sup> Many types of nonthermal atmospheric pressure plasma sources have been developed.<sup>[3]</sup> They can provide reasonable reactivity with a low gas temperature at atmospheric pressure. They are easy to construct because they do not need any vacuum system and can be operated with various feeding gases under a wide range of driving frequencies.

The discharge gaps, however, are usually limited to several centimeters due to the relative high breakdown voltage of working gases at atmospheric pressure.<sup>[2,8]</sup> The limitation of discharge gaps limits the size of materials to be treated, and consequently, the potential of atmospheric pressure plasma for various applications shrunk.<sup>[9]</sup> To address these concerns, non-equilibrium atmospheric pressure plasma jets have been attracting great interests.

H. W. Lee, J. K. Lee

Department of Electronic and Electrical Engineering, Pohang University of Science and Technology, Pohang, 790-784, Republic of Korea

S. H. Nam, G. C. Kim

Department of Oral Anatomy, School of Dentistry, Pusan National University, Yangsan, 626-810, Republic of Korea

Fax: 82-51-244-7399; E-mail: kig100om@pusan.ac.kr

A.-A. H. Mohamed

Department of Physics, Faculty of Science, Taibah University, Almadinah Almunawwarah, Saudi Arabia

A.-A. H. Mohamed

Department of Physics, Faculty of Science, Beni-Suef University, Beni-Suef, Egypt

Atmospheric pressure plasma jet devices generate plasma in surrounding air, so they are suitable for direct treatment of targets of any size.<sup>[2,9–11]</sup> Many different types of atmospheric pressure plasma jets were developed in a simple hand-held device with low cost.<sup>[2,8–13]</sup>

In the first part of this paper, the design of a finger-sized non-equilibrium atmospheric pressure plasma jet, which has suitable characteristics for various biomedical applications, and the study of its electrical and optical properties are described. To enhance the safety of the plasma jet without a loss of its reactivity, a floating inner electrode and a grounded outer electrode were equipped with the plasma jet. The inner electrode facilitates plasma ignition at low input voltage, and one of the outer electrodes prevents excessive current from flowing through a target (teeth or humans in this study) to be treated and enhances a reactivity of the plasma jet. The effects of additional electrodes and the optical properties of the plasma jet are demonstrated by voltage-current waveform measurement, electromagnetic modeling based on a finite element method and optical emission spectra analysis.

The rest of this paper demonstrates a tooth bleaching method with the plasma jet as a potential application. Nowadays dentists have interest in not only dental treatment, but also tooth esthetics. Because the beautiful appearance of teeth gives people confidence and fascination, tooth discoloration might induce mental pain, as well as deterioration of esthetics. Therefore, many patients look for dental assistance for improvement of discolored teeth. The cause of tooth discoloration is classified into extrinsic and internalized discoloration.<sup>[14–16]</sup> External chromogens such as coffee, wine and tobacco could stain or discolor the tooth enamel surface as extrinsic discoloration.<sup>[14–19]</sup> In dental clinic (in-office bleaching), high concentration of hydrogen peroxide ( $\text{H}_2\text{O}_2$ ) is used in combination with light sources. But substantial role of light sources has been

unclear and in a controversy.<sup>[20–22]</sup> Lee et al. showed that atmospheric pressure plasma in place of light sources showed effective tooth bleaching in weakly discolored teeth through tooth surface protein removal and increase of hydroxyl radical production.<sup>[23]</sup> In order to supply plasma device to dental clinic, further bleaching effect needs to be proved. Thus, one of the purposes of this study is to investigate whether the proposed plasma jet has a bleaching effect on strongly colored teeth with coffee or red wine. By combining plasma and  $\text{H}_2\text{O}_2$ , an enhanced tooth bleaching result is demonstrated.

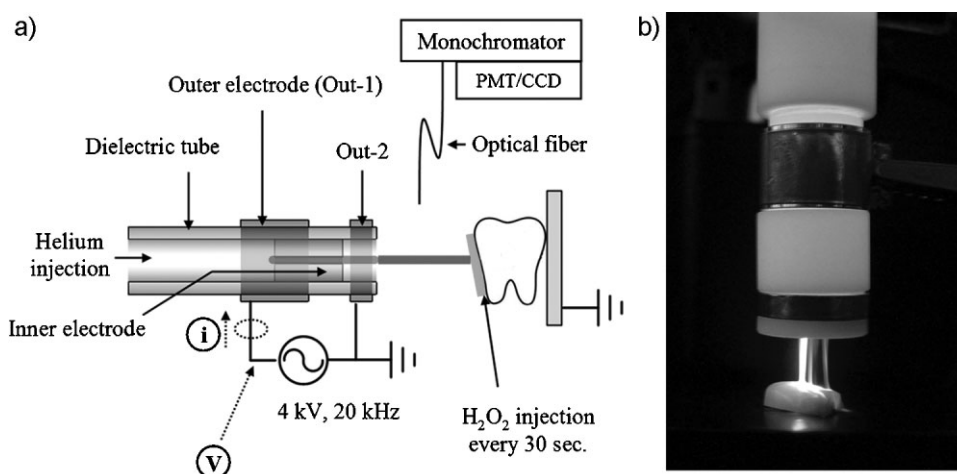
## Experimental Part

### Plasma Device

The plasma jet (Figure 1a) is driven by a low frequency (20 kHz) sinusoidal high voltage source (Dawonsys, MF Plasma Power Supply). The central dielectric tube (Teflon,  $\epsilon_r = 2.6$ ) has an inner diameter of 7 mm and an outer diameter of 9 mm. Two outer electrodes (aluminum) surround the dielectric tube and one floating inner electrode (aluminum) is inserted into the dielectric tube. One of the outer electrodes (Out-1) is connected to the high voltage source, and the other (Out-2) is connected to the ground. The inner electrode, which is not connected to any external power source (floating), is a cylinder perforated by several capillary holes of 1-mm diameter. Two different designs with and without the inner electrode were prepared. Helium gas with a flow rate of  $4 \text{ L} \cdot \text{min}^{-1}$  is used as feeding gas at atmospheric pressure in air.

### Plasma Diagnostics

Voltage was measured using a high voltage probe (Tektronix P6015A) and current was measured using a current probe (Pearson current monitor Model 4100, Figure 1a). The voltage and current signals were recorded by a digital oscilloscope (Tektronix DPO 4034). To investigate the effect of the floating inner electrode on the



■ Figure 1. a) Configuration of the tooth bleaching experiment and b) schematic of the plasma jet and of the process.

electric field intensity distributions and the gas breakdown voltage, a two dimensional finite element analyzer (Ansoft Maxwell 2D) was used. The cross sections of two different plasma jets with and without the inner electrode were modeled into a plane surface with its physical dimensions as described in the previous section. It was assumed that the inner cavity of the plasma jet is filled with air rather than helium gas.

For optical emission spectroscopy, a monochromator (Dong Woo Optron Co. Ltd., MonoRa-750i) equipped with a photomultiplier tube (PMT, R928 Hamamatsu) and a CCD camera (Andor Technology, DU401-BV) were used. Relative intensities of the optical emission line spectra of the discharge were taken at a distance of 2 cm from the plasma jet nozzle. The second positive nitrogen bands ( $C^3\Pi_u-B^3\Pi_g$ ,  $\Delta v = -2$ ) were measured to estimate the rotational temperature ( $T_{rot}$ ) and the vibrational temperature ( $T_{vib}$ ) of the plasma jet with a grating of  $2400\text{ mm}^{-1}$  blazed at 240 nm by using PMT. To identify the species generated by the plasma jet, optical emission spectra in the wavelength range of 200–900 nm were measured with a grating of  $150\text{ mm}^{-1}$  blazed at 500 nm by using the CCD camera.  $T_{rot}$  and  $T_{vib}$  were estimated by comparing modeled spectra with the measured spectra. The best fit conditions were obtained using the method described in ref.<sup>[24]</sup> The modeled spectra were calculated as a function of  $T_{rot}$  and  $T_{vib}$  in appropriate ranges. The root mean square error (RMSE) between measured and modeled spectra was used to find correspondence between them. The best fit point corresponds to the minimum RMSE.

### Tooth Bleaching Experiments and Analysis of Results

Thirty extracted human teeth were used for this experiment. Each tooth was cut in half longitudinally, and one half of each tooth was randomly assigned to either the experimental or the control group. Fifteen of the sectioned teeth were immersed in coffee (Maxim original - coffee subgroup) for seven days and fifteen were immersed in red wine (Palacio De Anglona Tinto Semidulce - red wine subgroup) for seven days. Before treatment, all the teeth were rinsed with distilled water to remove loose deposits on the teeth surfaces. Teeth in the experimental group were treated using  $\text{H}_2\text{O}_2$  (30 vol.-%, 20  $\mu\text{l}$  every 30 s) plus plasma (applied voltage: half the peak-to-peak amplitude = 4 kV) for 20 min (Figure 1b), and teeth in the control group were treated using  $\text{H}_2\text{O}_2$  alone for the same duration. For numerical analysis of bleaching results, photographs of the teeth were taken using a digital camera (Canon EOS Kiss Digital X with Canon MR-14EX Ring Flash and a 100-mm Canon Macro Lens EF). Teeth were photographed before treatment and at 5 min intervals during the 20 min treatment. Assessment of the color change of each tooth was based on the Commission Internationale de L'Eclairage (CIE) Lab Color System which is widely used for tooth color evaluation.<sup>[18,19]</sup> The overall color changes ( $\Delta E$ ) were calculated according to the following formula:

$$\Delta E = \sqrt{(\Delta L^*)^2 + (\Delta a^*)^2 + (\Delta b^*)^2} \quad (1)$$

where  $\Delta L^*$ ,  $\Delta a^*$  and  $\Delta b^*$  represent changes in lightness-darkness, redness-greenness and yellowness-blueness, respectively. The difference in color changes between experimental and control

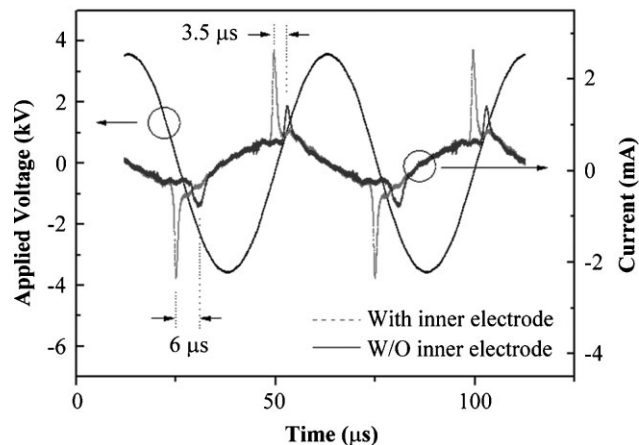


Figure 2. Measured waveforms of the applied voltage and the induced discharged current. Plasma parameters are: driving frequency = 20 kHz, applied voltage = 3.7 kV<sub>peak</sub>, helium flow rate = 4 L · min<sup>-1</sup>.

groups was tested using a paired *t* test. The change of  $\Delta E$  with time was calculated for each tooth, and then arithmetic means and standard deviations were calculated for each group (experimental and control groups of coffee and red wine subgroups).

## Results and Discussion

### Plasma Jet: Electrical Characteristics

Measured waveforms of applied voltage ( $V_a$ ) and total induced current ( $I_{total}$ ) (Figure 2) show the typical voltage-current waveform of a dielectric barrier discharge. The current  $I_{total}$  appears as a discharge current ( $I_{discharge}$ ) superimposed onto a displacement current ( $I_{displacement}$ ). The capacitive structure of the plasma jet makes the current  $I_{displacement}$  lead the applied voltage  $V_a$  by 90° in phase. The discharge current  $I_{discharge}$ , which stands for the effective gas breakdown, has much shorter duration than the excitation period (50  $\mu\text{s}$ ); and is observed once during every voltage rising (primary) and falling period (secondary). The discharge current  $I_{discharge}$  is caused by charge accumulation on the dielectric surface. These surface charge creates an electric potential that opposes the applied voltage and, as a result, limits the discharge current and prevents the glow-to-arc transition. At the same time, surface charge accumulated during one half-period favors the discharge breakdown in the next half-period.<sup>[3,12]</sup> The gas breakdown voltages of the two different designs, with and without the inner electrode, are compared. When the inner electrode is placed inside the dielectric tube as described (Figure 1), the discharge is ignited even at 3 kV<sub>peak</sub> (half the peak-to-peak amplitude) which is the minimum limitation of the voltage source used. On the other hand, the gas breakdown voltage of the discharge without the inner

electrode is  $3.6 \text{ kV}_{\text{peak}}$  which is higher than that in the case with the inner electrode. Current waveforms are plotted (Figure 2) for designs with and without the inner electrode at the same applied voltage of  $3.7 \text{ kV}_{\text{peak}}$  which is slightly higher than the gas breakdown voltage for the designs without the inner electrode. The discharge current  $I_{\text{discharge}}$  in the case with the inner electrode leads that in the case without the inner electrode by  $3.5 \mu\text{s}$  and  $6 \mu\text{s}$  in case of primary and secondary discharge current (i.e. when the applied voltage  $V_a$  is on the rise and fall), respectively. The peak current in the design that includes the inner electrode ( $2.6 \text{ mA}$ ) is much larger than that in without the inner electrode ( $1.4 \text{ mA}$ ). The plasma chemistry of the plume could be enhanced due to that increase in the discharge current.<sup>[9]</sup> This increment in the discharge current and its early appearance, in case of using the floating inner electrode, were similar to the effect of increasing the plasma jet discharge voltage which was reported earlier.<sup>[10]</sup> In this experiment, the same applied voltage was used for both cases, with and without inner electrode.

To make a close investigation into the effect of the inner electrode on the gas breakdown phenomenon, electric field intensity distributions for the two different designs of the plasma jet, with and without the inner electrode, are modeled (Figure 3). The maximum electric field intensities are  $8.13 \times 10^5 \text{ V} \cdot \text{m}^{-1}$  (with the inner electrode, Figure 3a) and  $3.75 \times 10^5 \text{ V} \cdot \text{m}^{-1}$  (without the inner electrode, Figure 3b) at the same applied voltage of  $3.7 \text{ kV}_{\text{peak}}$ . Even though the inner electrode is not connected to the any external power source or ground, it can increase the electric field intensity inside the plasma jet. As a result, it favors ignition of plasma at the lower applied voltage, which leads to early appearance of the discharge current and increases the discharge current. The conclusions drawn by the studies on gas breakdown voltage measurement, voltage-

current waveforms and modeling of an electric field intensity are well consistent: the improved plasma characteristics (the lowered gas breakdown voltage and enhanced reactivity, due to the increment in the discharge current), which can be observed with higher applied voltage, could be achieved by using the floating inner electrode while keeping the applied voltage at low level.

The effect of Out-2 was analyzed by applying a method similar to that described in ref.,<sup>[2]</sup> in which a simple electrical model was used to claim that the ground electrode limits the potential drop on the human body due to the presence of additional parallel current paths. In addition, enhanced reactivity of the plasma with a grounded electrode had been achieved.<sup>[12]</sup> Enhanced safety and reactivity of the suggested plasma jet are expected because the plasma jets are based on a similar structure to that used in ref. <sup>[2,12]</sup>

### Plasma Jet: Optical Characteristics

For biomedical applications of plasmas, low temperature plasma is required because most human tissues can be easily damaged by even weak thermal stimulation. A contour plot of RMSE as a function of modeled  $T_{\text{rot}}$  and  $T_{\text{vib}}$  (Figure 4a), the measured spectra and the corresponding best fit modeled spectra (Figure 4b) show excellent correspondence. Therefore,  $T_{\text{rot}}$  and  $T_{\text{vib}}$  could be estimated to be  $290 \text{ K}$  and  $2500 \text{ K}$ , respectively.  $T_{\text{rot}}$  is considered as the gas temperature of the plasma due to fast rotational-to-translational relaxation at atmospheric pressure.<sup>[24]</sup> The large difference between  $T_{\text{rot}}$  and  $T_{\text{vib}}$  shows that this plasma is in a highly non-equilibrium state which allows formation of abundant active ions and free radicals while maintaining a nonthermal characteristic.<sup>[24]</sup>

The emission spectra in the wavelength range of  $200\text{--}900 \text{ nm}$  revealed the presence of excited He,  $\text{N}_2$  and  $\text{N}_2^+$  in the plasma jet (Figure 5). In addition, atomic oxygen lines were detected. The atomic oxygen radical is a highly reactive radical and it can play important roles in biomedical applications of plasmas.<sup>[4,9,12,13,20,22]</sup>

### Tooth Bleaching

Coloration of teeth is affected by intrinsic and extrinsic stains.<sup>[14–16]</sup> Intrinsic tooth color is associated with the properties of the light scattering and absorption properties of the enamel and dentin.<sup>[14]</sup> Because most intrinsic stains cannot readily be removed, restorative techniques or chemical means such as peroxide are used to improve the intrinsic color.<sup>[16,19]</sup> The property of dentin plays a major role in determining the overall tooth color.<sup>[14,19]</sup> Dentin can be significantly discolored by a disease such as dental caries, so internal bleaching techniques of non-vital teeth have

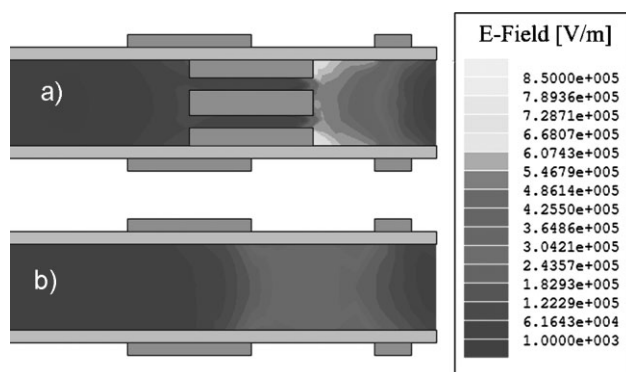


**Figure 3.** Modeled electric field intensity distributions inside the plasma jet a) with and b) without the inner electrode. Simulation conditions are: driving frequency =  $20 \text{ kHz}$ , applied voltage =  $3.7 \text{ kV}_{\text{peak}}$ . Air-filled cavity inside the plasma jet was assumed.

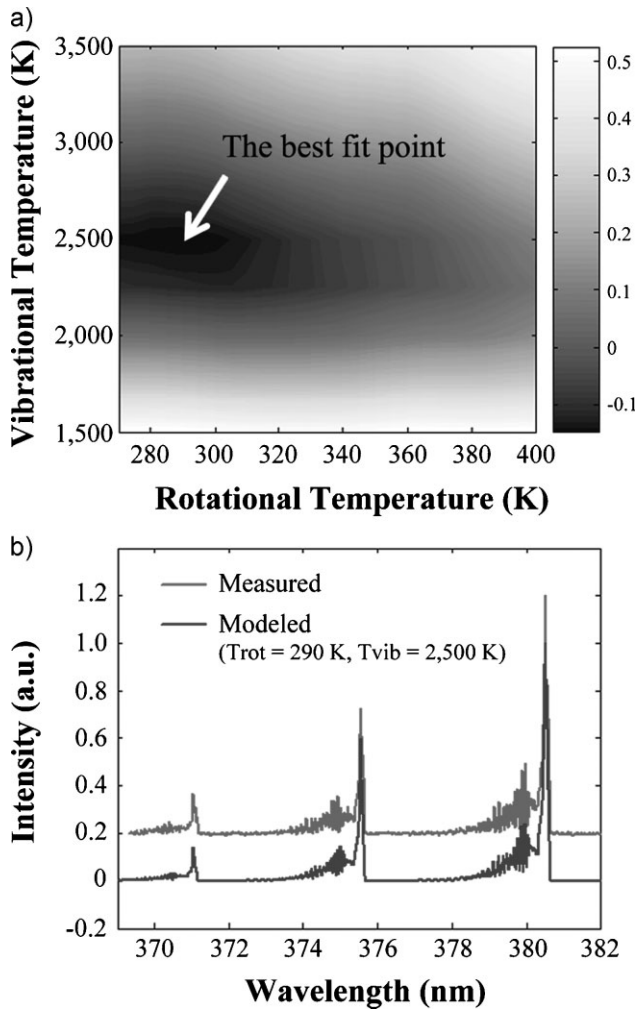


**Figure 4.** Determination of plasma temperatures, a) a contour plot of RMSE as a function of modeled  $T_{rot}$  and  $T_{vib}$  and b) spectra comparison between measured and modeled spectra at the best fit point ( $T_{rot} = 290\text{K}$ ,  $T_{vib} = 2\,500\text{K}$ ). Plasma parameters are: driving frequency = 20 kHz, applied voltage = 4 kV<sub>peak</sub>, helium flow rate = 4 L · min<sup>-1</sup>.

been used to treat dentin.<sup>[15]</sup> It was previously showed effective bleaching occurred within the dentin when H<sub>2</sub>O<sub>2</sub> and a plasma jet had been applied to it using sectioned extracted human teeth.<sup>[23]</sup>

On the contrary, extrinsic stains tend to be promoted on the enamel surface by smoking or dietary intake of tannin-rich foods such as coffee, red wine and tea.<sup>[14–19]</sup> Considering that the color-producing materials on a tooth surface are typically organic compounds that are adsorbed to the enamel surface,<sup>[14,25]</sup> it is helpful to remove or denature the proteins on teeth surface.<sup>[26]</sup> Plasma treatment was revealed to remove proteins on teeth surface, thereby it contributes to improvement in tooth bleaching.<sup>[23]</sup> In this study, the color of all the teeth was changed to dark brown due to staining with coffee or red wine for seven days. These stained teeth were significantly bleached by

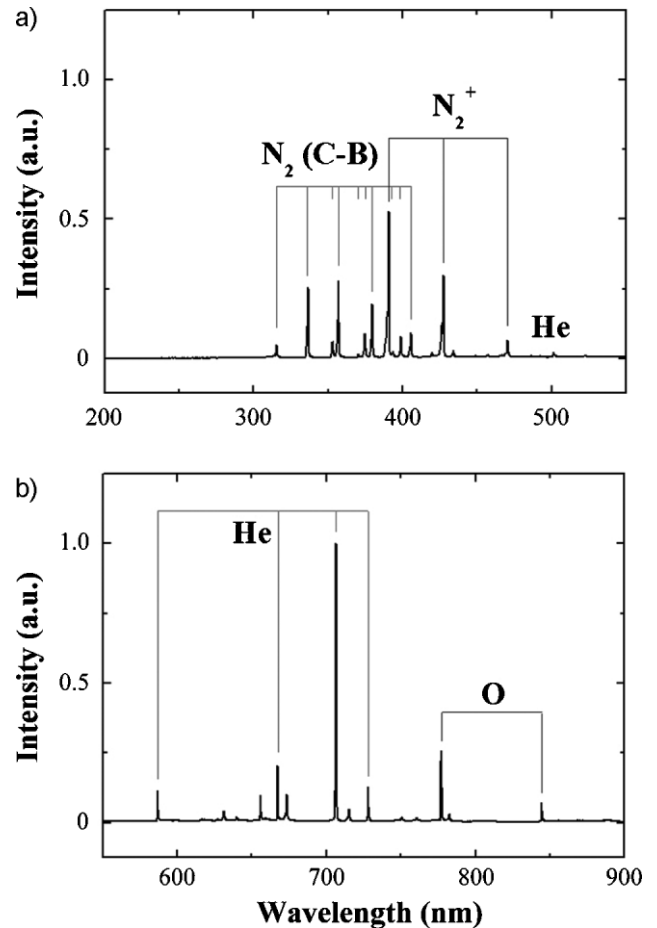


**Figure 5.** Measured emission spectra of the plasma plume: a) 200–550 nm range showing N<sub>2</sub>, N<sub>2</sub><sup>+</sup> and He lines; b) 550–900 nm range showing He and O lines. Plasma parameter are: driving frequency = 20 kHz, applied voltage = 4 kV<sub>peak</sub>, helium flow rate = 4 L · min<sup>-1</sup>.

plasma plus H<sub>2</sub>O<sub>2</sub> treatment compared with H<sub>2</sub>O<sub>2</sub> treatment alone in the manner of time dependence.

Remarkable color change occurred over time in the experimental group, whereas no significant color change occurred in the control group (Figure 6a). The differences in brightness and color tone between the experimental and control groups were significant after 20 min of treatment. The average overall color changes  $\Delta E \pm$  standard deviation were  $15.4 \pm 5.0$  (coffee) and  $26.0 \pm 8.8$  (red wine) for the experimental group, and  $5.0 \pm 2.2$  (coffee) and  $7.1 \pm 2.0$  (red wine) for the control group (Figure 6b).  $\Delta E$  for the experimental groups were 3.1 (coffee) and 3.7 (red wine) times larger than those of the corresponding control groups. P-values were 0.048 (coffee) and 0.009 (red wine). The differences between the experimental and control groups were significant for both subgroups ( $P < 0.05$ ). Because 20–30 min of whitening treatment is currently repeated for 3–4 weeks in office-bleaching, this result suggests that

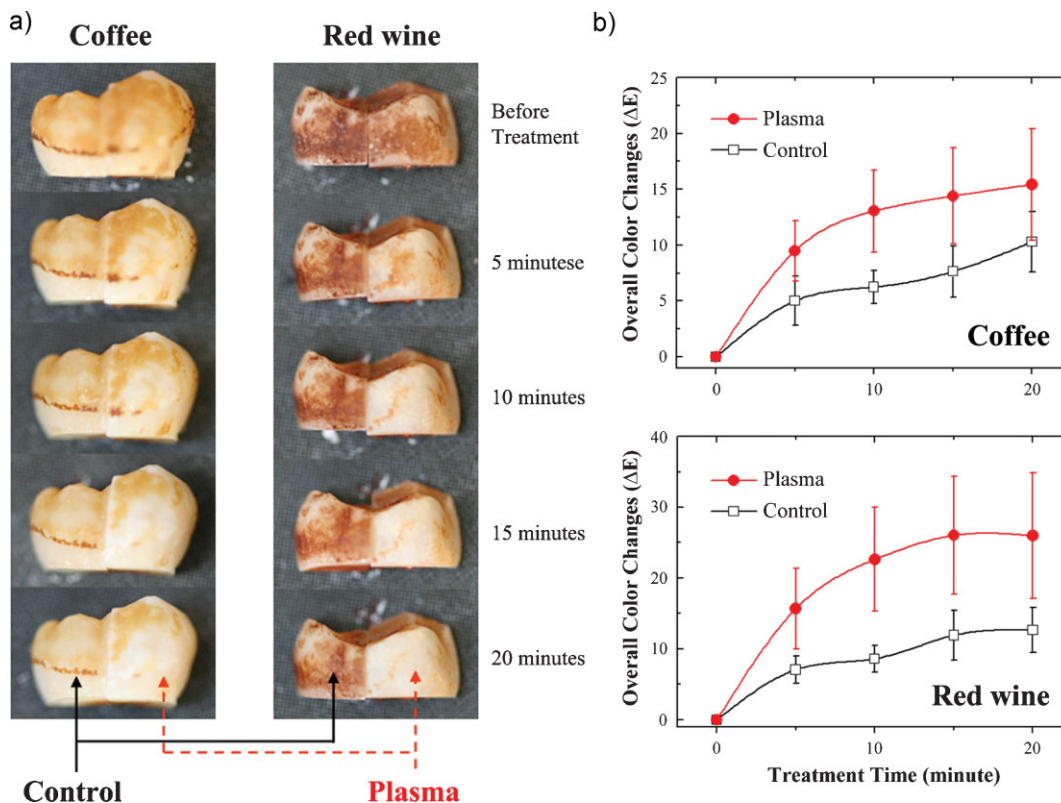


Figure 6. a) Photographs of tooth used before treatment and at every 5 min during the 20 min treatment. b) The change of overall color changes ( $\Delta E$ ) with time during the 20 min treatment.

plasma treatment could finish the tooth bleaching within very short time and lighten a burden imposed on patients.

Hydroxyl radical ( $\text{OH}^\bullet$ ) is widely known as the main substance responsible for tooth bleaching.<sup>[14,25–27]</sup> In our previous study, we showed that the production of  $\text{OH}^\bullet$  doubled after plasma treatment and claimed that this abundant  $\text{OH}^\bullet$  caused the enhanced tooth bleaching.<sup>[23]</sup> As a support experiment in this study, we tried to separate the tooth-bleaching effects of  $\text{H}_2\text{O}_2$  and plasma for 20 min, and the pH of the  $\text{H}_2\text{O}_2$  was recorded using a pH meter (Suntex SP-701 with Schott Instruments PH-Electrode). The  $\text{H}_2\text{O}_2$  had pH 3.1 before treatment and pH 2.7 after the 20-min treatment. In order to investigate whether the lowered pH induces bleaching effect, five teeth were immersed in the  $\text{H}_2\text{O}_2$  of pH 2.7 for 20 min, and their colors were assessed as described. In this case,  $\Delta E$  was not significantly different from that of the control group. This result indicates that tooth bleaching is caused by ions or free radicals that disappear right after plasma turn-off, not by lowered pH.  $\text{OH}^\bullet$  has also an extremely short lifetime ( $\approx 10^{-9}$  s),<sup>[28]</sup> so it can only be detected indirectly.<sup>[25–27]</sup> Therefore, this result is consistent with the hypothesis that  $\text{OH}^\bullet$  is responsible for tooth bleaching.

## Conclusion

This paper demonstrated a tooth bleaching effect of a non-equilibrium atmospheric pressure plasma jet that can be operated by a low frequency (20 kHz) high voltage source. The plasma jet consists of two outer electrodes, one inner electrode, and a dielectric tube. A helium plasma plume was clearly observed; this plume passes through the capillary holes of the inner electrode and extends up to 2 cm. Two different designs with and without the inner electrode resulted in different gas breakdown voltages. The plasma ignition voltage ( $< 3 \text{ kV}_{\text{peak}}$ ) in the design that includes the inner electrode case was slightly lower than that in the design without the inner electrode ( $3.6 \text{ kV}_{\text{peak}}$ ). Enhanced electric field intensity inside the plasma jet by the inner electrode which facilitates plasma ignition at low input voltage was proven through electromagnetic modeling based on a finite element method. The enhanced safety and reactivity of the plasma jet were achieved by using a grounded outer electrode. The  $T_{\text{rot}}$  and  $T_{\text{vib}}$  of the plasma jet were estimated to be  $\approx 290 \text{ K}$  and  $\approx 2500 \text{ K}$ , respectively. The large difference between them showed that the plasma jet was in a highly non-equilibrium state which allows formation of abundant ions and free radicals while

maintaining nonthermal characteristics. The presence of excited He, N<sub>2</sub>, N<sub>2</sub><sup>+</sup> and O in the plasma plume was revealed through the emission spectra measurement. The plasma jet was used in combination with H<sub>2</sub>O<sub>2</sub> to whiten the extracted teeth stained by either coffee or red wine. Combining the plasma jet and H<sub>2</sub>O<sub>2</sub> improved the bleaching efficacy by a factor of 3.1 (coffee) and 3.7 (red wine) compared with using H<sub>2</sub>O<sub>2</sub> alone. The proposed tooth bleaching method using atmospheric pressure plasma jet shows reasonable promise of being practical.

**Acknowledgements:** This work was supported by the *Korea Science and Engineering Foundation (KOSEF)* grant (No. R01-2007-000-10730-0) and the *Brain Korea 21* program funded by the *Korea Ministry of Education, Science and Technology*. The authors are grateful to Dr. *Jeong Kil Park* for his comments and Dr. *XinPei Lu* for providing us his temperature simulation program.

Received: May 31, 2009; Revised: August 14, 2009; Accepted: September 30, 2009; DOI: 10.1002/ppap.200900083

**Keywords:** atmospheric pressure plasmas; optical emission spectroscopy (OES); peroxides; plasma jets; tooth bleaching; whitening

- [1] F. Iza, J. K. Lee, M. G. Kong, *Phys. Rev. Lett.* **2007**, *99*, 075004.  
[2] X. Lu, Z. Jiang, Q. Xiong, Z. Tang, X. Hu, Y. Pan, *Appl. Phys. Lett.* **2008**, *92*, 081502.  
[3] F. Iza, G. J. Kim, S. M. Lee, J. K. Lee, J. L. Walsh, Y. T. Zhang, M. G. Kong, *Plasma Process. Polym.* **2008**, *5*, 322.  
[4] M. Laroussi, *Plasma Process. Polym.* **2005**, *2*, 391.  
[5] S. U. Kalghatgi, G. Fridman, M. Cooper, G. Nagaraj, M. Pedinghaus, M. Balasubramanian, V. N. Vasilets, A. F. Gutsol, A. Fridman, G. Friedman, *IEEE Trans. Plasma Sci.* **2007**, *35*, 1559.  
[6] G. Fridman, G. Friedman, A. Gutsol, A. B. Shekhter, V. N. Vasilets, A. Fridman, *Plasma Process. Polym.* **2008**, *5*, 503.  
[7] [7a] G. C. Kim, G. J. Kim, S. R. Park, S. M. Jeon, H. J. Seo, F. Iza, J. K. Lee, *J. Phys. D: Appl. Phys.* **2009**, *42*, 032005; [7b] G. C. Kim, G. J. Kim, S. R. Park, S. M. Jeon, H. J. Seo, F. Iza, J. K. Lee, *Europhys. News* **2009**, *40*, 14.  
[8] A. Schütze, J. Y. Jeong, S. E. Babayan, J. Park, G. S. Selwyn, R. F. Hicks, *IEEE Trans. Plasma Sci.* **1998**, *26*, 1685.  
[9] X. Lu, Z. Jiang, Q. Xiong, Z. Tang, Y. Pan, *Appl. Phys. Lett.* **2008**, *92*, 151504.  
[10] Q. Xiong, X. Lu, K. Ostrikov, Z. Xiong, Y. Xian, F. Zhou, C. Zou, J. Hu, W. Gong, Z. Jiang, *Phys. Plasmas* **2009**, *16*, 043505.  
[11] M. Teschke, J. Kedzierski, E. G. Finantu-Dinu, D. Korzec, J. Engemann, *IEEE Trans. Plasma Sci.* **2005**, *33*, 310.  
[12] S. J. Kim, T. H. Chung, S. H. Bae, S. H. Leem, *Appl. Phys. Lett.* **2009**, *94*, 141502.  
[13] Y. C. Hong, H. S. Uhm, *Appl. Phys. Lett.* **2006**, *89*, 221504.  
[14] A. Joiner, *J. Dent.* **2006**, *34*, 412.  
[15] A. Watts, M. Addy, *Br. Dent. J.* **2001**, *190*, 309.  
[16] M. Addy, J. Moran, *Adv. Dent. Res.* **1995**, *9*, 450.  
[17] S. B. Berger, A. S. Coelho, V. A. P. Oliveira, V. Cavalli, M. Giannini, *J. Appl. Oral Sci.* **2008**, *16*, 201.  
[18] P. Villalta, H. Lu, Z. Okte, F. Garcia-Godoy, J. M. Powers, *J. Prosthet. Dent.* **2006**, *95*, 137.  
[19] M. Moore, N. Hasler-Nguyen, G. Saroea, *BMC Oral Health* **2008**, *8*, 23.  
[20] K. Luk, L. Tam, M. Hubert, *J. Am. Dent. Assoc.* **2004**, *135*, 194.  
[21] M. Tavares, J. Stultz, M. Newman, V. Smith, R. Kent, E. Carpino, J. M. Goodson, *J. Am. Dent. Assoc.* **2003**, *134*, 167.  
[22] A. H. Jones, A. M. Diaz-Arnold, M. A. Vargas, D. S. Cobb, *J. Esthet. Dent.* **1999**, *11*, 87.  
[23] H. W. Lee, G. J. Kim, J. M. Kim, J. K. Park, J. K. Lee, G. C. Kim, *J. Endod.* **2009**, *35*, 587.  
[24] D. Staack, B. Farouk, A. F. Gutsol, A. Fridman, *Plasma Sources Sci. Technol.* **2006**, *15*, 818.  
[25] M. Kashima-Tanaka, Y. Tsujimoto, K. Kawamoto, N. Senda, K. Ito, M. Yamazaki, *J. Endod.* **2003**, *29*, 141.  
[26] K. Kawamoto, Y. Tsujimoto, *J. Endod.* **2004**, *30*, 45.  
[27] K. Sakai, J. Kato, H. Kurata, T. Nakazawa, G. Akashi, A. Kameyama, Y. Hirai, *Laser Phys.* **2007**, *17*, 1062.  
[28] S. Cheng, W. Fung, K. Chan, P. K. Shen, *Chemosphere* **2003**, *52*, 1797.